Clim Dyn
DOI 10.1007/s00382-017-3582-4

Subseasonal prediction of the heat wave of December 2013 in Southern South America by the POAMA and BCC-CPS models

Marisol Osman[1,2] · **Mariano S. Alvarez**[1,2]

Received: 1 September 2016 / Accepted: 9 February 2017

Abstract The prediction skill of subseasonal forecast models is evaluated for a strong and long-lasting heat wave occurred in December 2013 over Southern South America. Reforecasts from two models participating in the WCRP/WWRP Subseasonal to Seasonal project, the Bureau of Meteorology POAMA and Beijing Climate Center model BCC-CPS were considered to evaluate their skill in forecasting temperature and circulation anomalies during that event. The POAMA reforecast of 32-member ensemble size, initialized every five days, and BCC-CPS reforecast of 4-member ensemble size for the same date of POAMA plus the previous 4 days were considered. Weekly ensemble-mean forecasts were computed with leadtimes from 2 days up to 24 days every 5 days. Weekly anomalies were calculated for observations from 13th of December to 31st of December 2013. Anomalies for both observations and reforecast were calculated with respect to their own climatology. Results show that the ensemble mean warm anomalies forecasted for week 1 and 2 of the heat wave resulted more similar to the observations for the POAMA model, especially for longer leads. The BCC-CPS performed better for leads shorter than 7 (14) for week 1 (2). For week 3 the BCC-CPS outperformed the POAMA model, particularly at shorter leads, locating more accurately the maxima of the anomalies. In a probabilistic approach, POAMA predicted with a higher chance than BCC-CPS the excess of the upper tercile of temperature anomalies for almost every week and lead time. The forecast of the circulation anomalies over South America could be used to explain the location of the highest temperature anomalies. In summary, for this case, models skill in forecasting surface temperature in a context of a heat wave resulted moderate at lead times longer than the fortnight. However, this study is limited to model-to-model analysis and a multi-model ensemble strategy might increase the skill.

Keywords S2S · South America · SACZ · Heat wave

1 Introduction

During December 2013 a persistent heat wave affected the central-northern sector of Argentina as well as the northern Patagonia region. On December 11 the temperature started to rise over the central region of Argentina and by December 19 the region with high temperatures spanned to the northern sector of Argentina while temperature anomalies intensified in the central portion. Maximum and minimum temperatures were over the 90th percentile between 5 and 18 days over the region affected by the heat wave and attained a record for some ground stations (Cerne et al. 2015; SMN 2014). Due to the persistence of high temperature values the energy consumption reached a historical record increasing 13.4% with respect to the previous year. The high demand for electricity led to a blackout that affected near 1M of the population and, to save electricity, the local and national governments gave a day off to their employees (Barros et al. 2015).

The work of Cerne et al. (2015) provides an overview of the circulation anomalies during the event and the role

✉ Marisol Osman
osman@cima.fcen.uba.ar

[1] Departamento de Ciencias de la Atmósfera y los Océanos, Facultad de Ciencias Exactas y Naturales, Universidad de Buenos Aires, Buenos Aires, Argentina

[2] Centro de Investigaciones del Mar y la Atmósfera (CIMA), Instituto Franco Argentino sobre Estudios de Clima y sus Impactos (UMI IFAECI)/CNRS, CONICET - Universidad de Buenos Aires, Buenos Aires, Argentina

Published online: 04 March 2017

of the intraseasonal variability in the modulation of those anomalies. According to the authors, the development of anticyclonic anomalies promoted adiabatic subsidence and clear skies favoring the diabatic heating. The South Atlantic Convergence Zone (SACZ) is a convective band that spans a region over the Amazon Basin towards the southeast into the south Atlantic Ocean, and its activity has been linked to the development of most of the persistent heat waves over southern South America (Cerne and Vera 2011). In particular, the heat wave under analysis started during an active phase (enhanced convection) of the SACZ, hereafter, a SACZ event, and by the end of the heat wave the circulation favored the presence of northerly wind, increasing the temperature and moisture advection (Cerne et al. 2015). The authors also showed that the leading mode of intraseasonal variability of outgoing longwave radiation (OLR) over South America during the warm season, which presents a dipole-like structure with centers of action over the SACZ region and southeastern South America (SESA) (e.g., Gonzalez and Vera 2014) was active during the heat wave, reflecting the influence of intraseasonal activity in the evolution of the observed temperature anomalies. This heat wave was studied from different approaches, such as dynamical (Cerne et al. 2015) and climatic change detection and attribution (Hannart et al. 2015); however, to the date there are no works which address the ability of models in forecasting this event.

Recently, the World Weather Research Programme (WWRP) and the World Climate Research Programme (WCRP) implemented the Subseasonal to Seasonal project (S2S) with the main goal of improving forecast skill and understanding on the subseasonal to seasonal timescale with special emphasis in high-impact weather events (Vitart et al. 2016). To achieve this objective, an archive of retrospective forecasts produced with state-of-the-art Coupled Global Circulation Models (CGCMs) from different climate prediction centers was prepared. The availability of this dataset provides a unique opportunity to examine prediction skill of extreme events on timescales beyond the medium-range weather, as well as to study the representation of climate anomalies that favored the occurrence of those events. This kind of study has been conducted in other regions, e.g. Marshall and Hendon (2015), Wu et al. (2016), but has not been done for South America yet.

The aim of this work is to assess the performance of two models participating in the S2S project (POAMA and BCC-CPS) in forecasting the heat wave of December 2013 occurred in Southern South America. Special emphasis is made in evaluating the ability of models in forecasting temperature and circulation anomalies for leadtimes longer than the fortnight. This paper is organized as follows: Sect. 2 describes the models and methodology used to assess the skill; Sect. 3 discusses the skill achieved by the models. Finally, Sect. 4 presents the conclusions.

2 Data and methodology

Reforecast from two models participating in the WWRP/WCRP Subseasonal to Seasonal project, the Bureau of Meteorology POAMA and Beijing Climate Center Climate Prediction System version 1 (BCC-CPS) were considered to evaluate their skill in forecasting temperature and circulation anomalies. These models were selected among those available as their reforecast period span the year of the event. Although the ECMWF model also spans 2013 in its reforecast, it was not considered in this study as the performance of the models was analyzed respect to the daily ERA Interim reanalysis (Dee et al. 2011), thereby avoiding a potential bias to better results. For each model, 2 m temperature and outgoing longwave radiation (OLR) were used to describe the regional conditions and the 200 hPa geopotential height to analyze the associated hemispheric circulation. In the case of OLR, it was compared to NOAA interpolated satellite estimates (Liebmann and Smith 1996).

POAMA model is a coupled ocean–atmosphere climate model that uses the Bureau of Meteorology Research Centre Atmospheric Model (BAM3.0) for the atmosphere and the Australian Community Ocean Model version 2 (ACOM2) for the ocean (Cottrill et al. 2013 and references therein). Forecasts are initialized from the PEODAS (POAMA Ensemble Ocean Data Assimilation System, Yin et al. 2011) and comprises a 33 member ensemble: one control simulation and 32 members generated using coupled breed vectors (Hudson et al. 2013). The POAMA S2S database consists of real-time forecasts from BoM from 1st January 2015, and the full set of re-forecasts run 6 times a month (1st, 6th, 11th, 16th, 21st, 26th of each month) from 1981 to 2013. The BCC-CPS is based on the fully-coupled BCC Climate System Model BCC-CSM1.2 (Liu et al. 2016). The atmospheric model is an adaptation of the Community Atmosphere Model version 3 developed at the National Center for Atmospheric Research (Wu 2012) while the ocean component is the National Oceanic Atmospheric Administration (NOAA) GFDL Modular Ocean Model version 4 (MOM4; Griffies et al. 2005). Forecasts are initialized from the BCC Coordinated Initialization System (CIS) and consist of 4 ensemble members generated using the lagged average forecasting technique, which are initialized at 00 UTC of the first forecast day and 18, 12 and 06 UTC of the previous day, respectively. The BCC-CPS S2S database runs on every day and ends with a 60-day integration. Re-forecasts go from 1994 to 2013 while real-time forecasts are from 1st January 2015.

The analysis of temperature and circulation anomalies was performed weekly for the period from December 13 up to December 31 of 2013, which was defined by Cerne et al. (2015) as the period encompassing the heat wave. Week 1 of the heat wave spans December 13 to 19, week 2 December 20 to 26, while the last week of the heat wave spans only 5 days, from December 27 to 31, to complete the period. The POAMA reforecast of 32-member ensemble size, which are the perturbed forecast initialized every five days, and the BCC-CPS reforecast of 4-member ensemble size for each day were considered. The BCC-CPS ensemble was constructed using the forecast of the same date as POAMA plus the previous 4 days resulting in a 20 ensemble-member forecast. The ensemble mean forecast for each of the 3 weeks of the heat wave is computed with leadtimes from 2 days up to 22 days every five days. Weekly anomalies were calculated for both observations and reforecast with respect to their own climatology for 1994–2012 which, in the case of the forecast, is a function of both, date of the forecast and leadtime. The statistical significance of those anomalies was evaluated comparing the forecasted ensemble mean for each lead and week and the climatological mean for that week using a test for differences of mean, following Wilks (2011). In this study, we only plot and describe anomalies significant at the 95% confidence level.

The performance of the models was assessed deterministically computing the following spatial verification scores:

Mean Error:

$$ME = \frac{1}{n}\sum_{i=1}^{n}|\widehat{x_i} - x_i| \tag{1}$$

Root Mean Square Error:

$$RMSE = \sqrt{\frac{1}{n}\sum_{i=1}^{n}(\widehat{x_i} - x_i)^2} \tag{2}$$

and Anomaly Correlation Coefficient:

$$ACC = \frac{\sum_{i=1}^{n}(\widehat{x_i'} - \overline{\widehat{x}'})(x_i' - \overline{x'})}{n\sqrt{\frac{\sum_{i=1}^{n}(\widehat{x_i'} - \overline{\widehat{x}'})^2}{n}\frac{\sum_{i=1}^{n}(x_i' - \overline{x})^2}{n}}} \tag{3}$$

In all cases x represents mean weekly observations, $\widehat{x}$ mean weekly forecast and i represents grid points, whereas overbar denotes spatial mean and primes refers to departures from the climatology (Brown et al. 2011). All the metrics were computed for the ensemble mean and for each ensemble member.

On the other hand, the forecasts were also evaluated using a probabilistic approach. As it was pointed out in the introduction, extreme temperatures were observed during the event in most of the region. For this reason, for each model and each grid point we computed the probability of exceeding the weekly 75th percentile. The percentile value, which is a function of the week of the forecast and the leadtime, is computed using the ensemble mean forecast between 1994 and 2012 while the forecasted probabilities were obtained calculating the fraction of the ensemble members with values higher than the percentile.

3 Results

3.1 Temperature

The observed weekly temperature anomalies and the forecast for different lead times are presented in Figs. 1, 2 and 3. The associated spread for each model and lead time was also computed (not shown). Additionally, the evolution of the skill scores for the ensemble mean and each member for each week averaged over the boxes outlined in the observation maps is presented in Fig. 4. During week 1 of the heat wave, positive weekly-averaged temperature anomalies were observed over most of southern, central and northeastern Argentina, southern Brazil and Uruguay, with maxima over northern Patagonia and central Argentina of over 5 °C (Fig. 1). The POAMA model was able to forecast a weak positive anomaly in northern Patagonia for lead 22 and expanded it to central and eastern Argentina for lead 17, correctly spanning the region affected by the heat wave but with less intensity. The most intense anomaly forecasted by the POAMA model was for lead 12 located over central Argentina, reaching 5 °C over northern Patagonia with a spread of 3 °C. This forecasted anomaly decreased its amplitude for lead 7 and was located over central Argentina and southeastern Brazil for lead 2, where it only reached 2 °C with a spread of 2 °C. The BCC-CPS model forecasted for every lead but 12 the more intense warm anomalies near the Andes Cordillera, and cold anomalies over northeastern Argentina, southern Brazil and Paraguay, which were not observed in week 1. The forecasted anomaly was located mainly over the Patagonia region for leads 22, 17 and 7, the latter reaching 3 °C with a spread of around 2 °C. Differently, the model forecasted for lead 12 the anomaly over northern Argentina and for lead 2 over northern Patagonia and central-western Argentina (Fig. 1). Another feature observed during week 1 are the weak cold anomalies over the southwestern Atlantic Ocean which were detected only since lead 7 by the POAMA model and were not forecasted by the BCC-CPS model (Fig. 1). Comparing the skill scores to those achieved by the ensemble mean of POAMA model, the ensemble mean of BCC-CPS had a worse performance in the prediction of the first week of the heat wave, with a more negative ME for all leads but for lead 2, when it became slightly lower than POAMA's ME, a higher RMSE and lower ACC (Fig. 4). The ME values

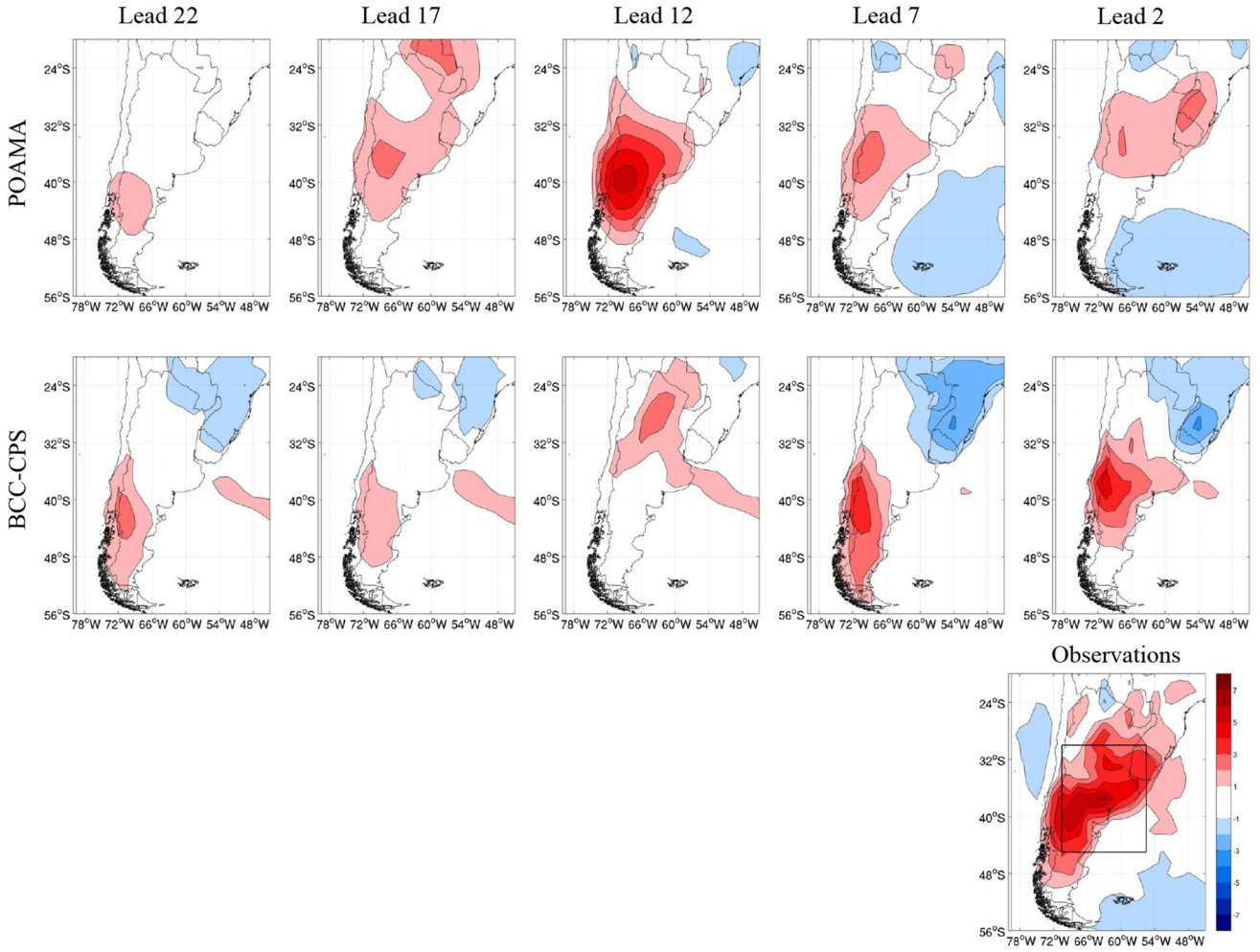

Fig. 1 Reforecasts of weekly-averaged 2-m air temperature anomalies for POAMA model (*up*) and BCC-CPS (*down*) for week 1 of the heat wave (13 to 19 of December of 2013). The lead time indicates how many days before of the 1st day of the week the forecast started. Observations for week 1 are shown at the *bottom-right*. The *box in a thick contour* indicates the area selected for computing the skill scores. Units are in °C

for this week show that POAMA ensemble mean underestimated the magnitude of the heat wave for every lead time, while the RMSE shows that the model performed better for lead 12 (Fig. 4). The ACC resulted greater than 0.4 for every lead time, and was higher than 0.75 for leads 17 and 12. The evolution of the scores for the ensemble mean of BCC-CPS model was overall to the better for shorter lead times, while the POAMA scores resulted better for lead 12 and not as good for longer and shorter lead times (Fig. 4). In addition, while the spread in the scores reduced with shorter leadtimes for BCC-CPS ensemble members, the performance of the POAMA ensemble was almost insensitive to leadtimes.

During the week 2 of the heat wave, warm temperature anomalies were observed over most of Argentina, and also over Uruguay and southern Brazil, with one maximum located over northern Patagonia and another one over central Argentina between 27S and 39S (Fig. 2). The POAMA model forecasted warm anomalies over central Argentina and SESA for every lead time considered, though, when compared to the observed anomalies, it mostly captured the maximum over northern Patagonia and Buenos Aires province but not between 27S and 35S. The forecasts of the BCC-CPS model for lead times 24 and 19 did not show large regions of warm anomalies over southern South America (Fig. 2). For lead 14, 3 °C anomalies with a 1 °C spread were forecasted for the northern and western Patagonia, while no anomalies were forecasted to the north. The model detected the warm anomalies over Argentina and Uruguay only 9 days before the start of week 2, anomalies which resulted quite weaker than those observed. For lead 4, however, the BCC-CPS model was able to predict warm anomalies for week 2 of the heat wave, with maxima of up to 5 °C in northern

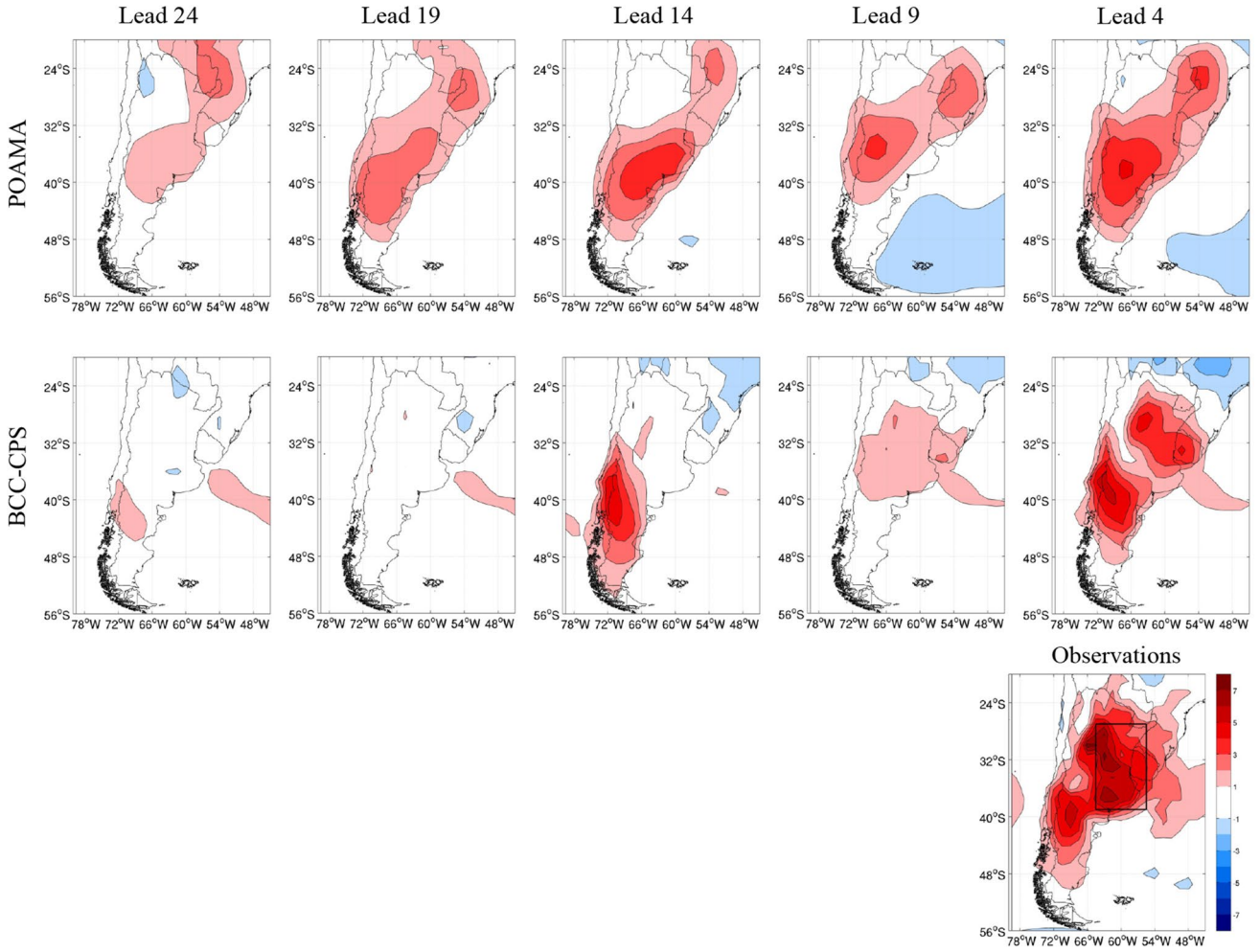

Fig. 2 As Fig. 1 but for week 2 of the heat wave (20 to 26 of December of 2013)

Patagonia and 4 °C over central Argentina north of 32S, both corresponding to observed regions of maxima (Fig. 2) and with a spread of 1 °C in the region (not shown). The associated skill scores show for POAMA that the ME of the ensemble mean remained practically constant, reflecting the underestimation of the warm anomalies between 2 and 3 °C for the analyzed lead times (Fig. 4). This behavior was accompanied by most of the ensemble members. The RMSE of the ensemble mean achieved values in between 3.5 and 3 °C, decreasing to 2.5 °C for the shortest lead time (Fig. 4), when the more intense anomalies were forecasted for central Argentina (Fig. 2). However, some ensemble members had two or three times higher RMSE than that for the ensemble mean. The ACC of the ensemble mean resulted in 0.4 for leads 19 and shorter, showing the consistency of the POAMA forecast of the heat wave. Even though, some ensemble members presented negatives ACC for most of the leadtimes and consequently the mean of the ACC for the ensemble is non-significant for all the leadtimes. BCC-CPS ensemble mean's ME and RMSE were worse than POAMA's until lead 9, when a substantial improvement was made: the ensemble mean ME (RMSE) was reduced to °C (3.1 °C) and then to −1.5 °C (2.1 °C) for lead 4. The BCC-CPS ensemble members showed a reduction in the spread of the skill scores towards shorter leadtimes. The ACC for the ensemble mean BCC-CPS model also improved considerably with shorter lead times, being greater than POAMA's ACCs for lead times 14 and shorter. In addition, the ensemble members also improved the ACC for short leadtimes being the mean of all of them significant for leads 9 and 4. It should be noted that although BCC-CPS outperformed POAMA regarding the skill scores in the region of analysis for leads 9 and especially 4, qualitatively the patterns of anomalies forecasted by POAMA seemed overall more accurate than those forecasted by BCC-CPS (Fig. 2).

During week 3 of the heat wave warm anomalies displaced northward to northern Argentina and SESA,

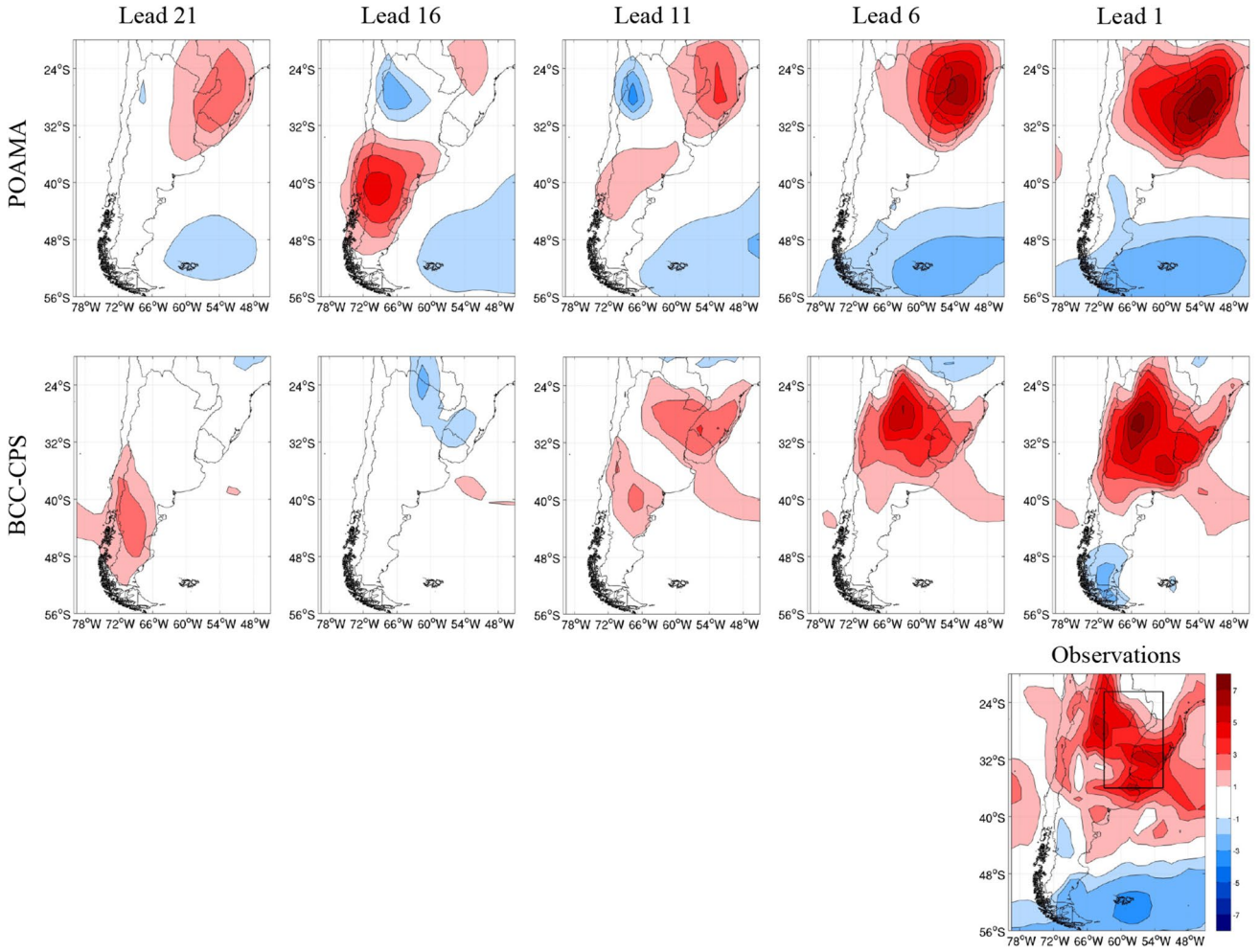

Fig. 3 As Fig. 1 but for week 3 of the heat wave (27 to 31 of December of 2013)

with maxima over Uruguay, the coast of Argentina at around 36S and also northern-central Argentina near 28S (Fig. 3). For every lead time, the POAMA model forecasted positive anomalies over SESA, which expanded to the west for leads 6 and 1 though maximizing over southern Brazil, north of the maximum observed (Fig. 3). The model forecasted warm anomalies over northern Patagonia 16 days prior to the start of week 3 along with cold anomalies in the northwest of Argentina, but those anomalies were not forecasted for leads shorter than 11. The forecast for week 3 of the BCC-CPS model was of warm anomalies over the Patagonian region for lead 21, however, it improved since lead 11: warm anomalies were forecasted over northern Argentina and SESA, with maxima over central Argentina around 28S and also eastern Argentina at 35S since lead 6 (Fig. 3). The skill scores for the POAMA model resulted as expected, as the forecast was worse for lead 16, and improved since then, obtaining an approximately 0 °C ensemble mean ME for lead 6 and about 1.2 °C of overestimation for lead 1 (Fig. 4). The evolution of the ME for the ensemble members changed from negative for most of them for long leadtimes to positive for most of them for the shortest leadtime. The RMSE of the ensemble mean descended from 3.4 °C for lead 16 to 2.7 °C for lead 11 and 2.4 °C for lead 1 while the RMSE for the ensemble members considerably reduced its spread and diminished towards shorter leadtimes. On the other hand, the ACC resulted negative and higher for leads 16 and 11, reaching positive values of around 0.2 only for lead 1. The POAMA ensemble members showed a better performance than the ensemble mean for most of the leadtimes, especially the longer ones. All skill scores for the ensemble mean of BCC-CPS model improved—and outperformed the ensemble mean of POAMA model—since lead 11: ME changed from −1.5 °C to almost 0 °C for lead 1, the RMSE descended from 2 to 1.25 °C and the ACC reaching values around 0.6 to 0.8 (Fig. 4). In addition, most of

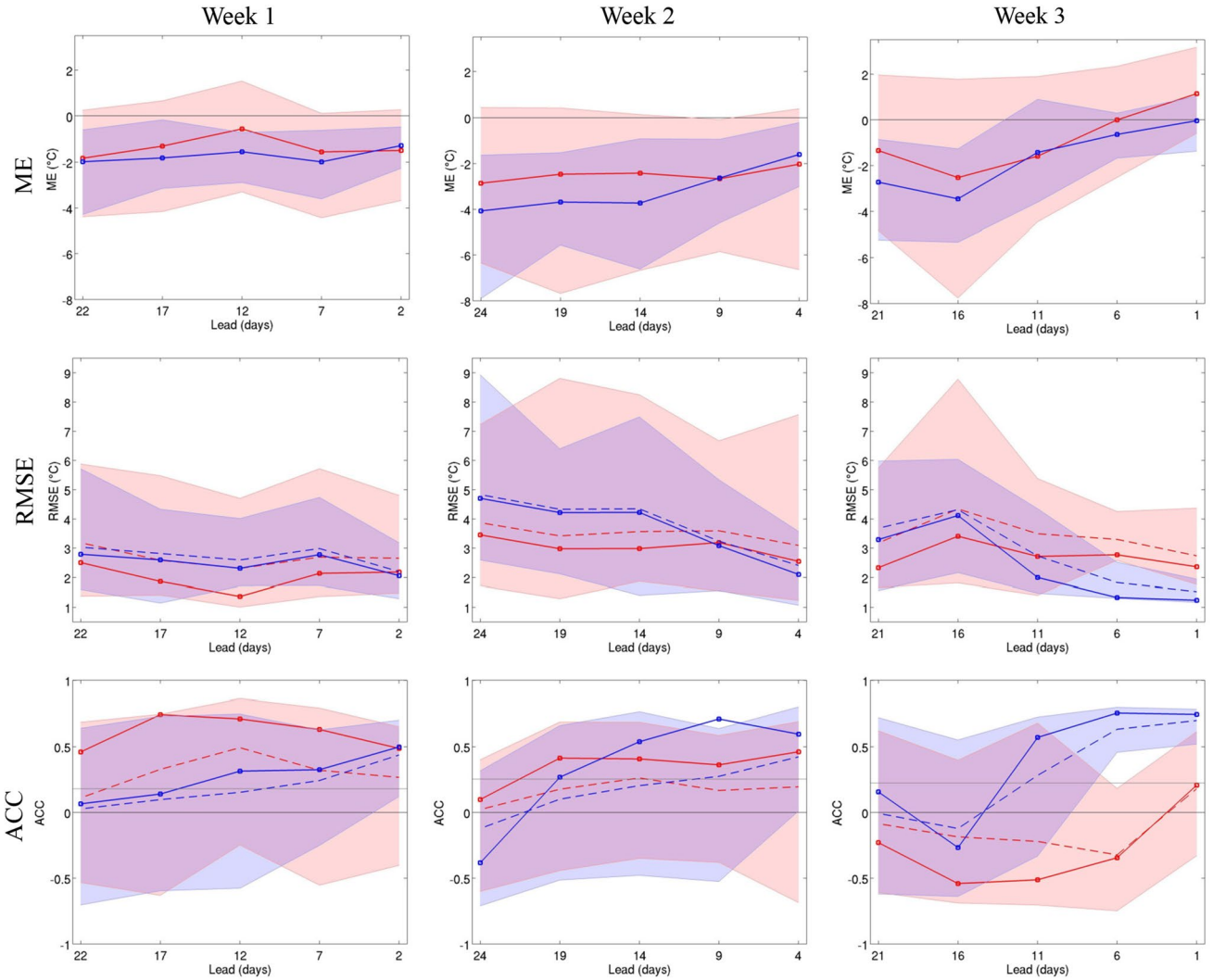

Fig. 4 Skill scores for the ensemble mean (*solid line*), the ensemble members (*shaded*) and the mean scores for the ensemble members (*dashed line*) of POAMA (*red*) and BCC-CPS (*blue*) models for the three weeks of analysis. From *top to bottom*: Mean Error (in °C), Root Mean Square Error (in °C), Anomaly Correlation Coefficient

the BCC-CPS ensemble members outperformed POAMA ensemble members in terms of RMSE and ACC for lead-times 6 and 1.

Additionally, cold anomalies were observed over the southwestern Atlantic Ocean and the southern tip of the continent during this week, which led to the end of the heat wave in the Patagonia region. These cold anomalies were detected since lead 21 by the POAMA model, locating the anomaly center more to the west for shorter lead times (Fig. 3), and were not forecasted by the BCC-CPS, though negative anomalies were forecasted over southern Patagonia for lead 1.

Besides analyzing the deterministic forecast by the ensemble mean for both models, a probabilistic approach was also taken. Observed weekly anomalies were above the 75th percentile for the entire event. Therefore, for each week of the heat wave we computed the probability of exceeding that percentile of the weekly-averaged temperature anomalies, which is nominally 25%, within the boxes selected for each week (Table 1). For week 1, the POAMA model showed a higher than nominal chance for leads 22 and 12, reaching 50% of probability for the latter. The probability was higher than nominal for leads 17, 12 and 2 for the BCC-CPS, and it was highest for lead 17. The POAMA model showed a probability of exceeding the 75th percentile higher than 56% for all leads during week 2, while the BCC-CPS only exceeded the nominal probability for leads 9 and 4. In the same way, POAMA forecasted with a higher than nominal probability for each lead for week 3, even with a 56% chance for lead 21. Again, the BCC-CPS model only got to forecast a higher than nominal probability since lead 11. Therefore, the results show that the POAMA

Table 1 Probability of exceeding the 75th percentile for weekly-averaged temperature forecasted by POAMA and BCC-CPS models in the according boxes of analysis

Week1	Lead 22	Lead 17	Lead 12	Lead 7	Lead 2
POAMA	28	19	50	16	6
BCC-CPS	25	50	40	0	30
Week2	Lead 24	Lead 19	Lead 14	Lead 9	Lead 4
POAMA	56	59	56	63	56
BCC-CPS	15	25	15	65	75
Week3	Lead 21	Lead 16	Lead 11	Lead 6	Lead 1
POAMA	56	31	41	81	100
BCC-CPS	15	10	45	80	95

Values are in %

model outperformed the BCC-CPS model in the probabilistic long-lead forecast of the high temperatures during the heat wave.

As the development of an upper-level anticyclonic anomaly in Southern South America, embedded in a Rossby wavetrain extended along the South Pacific Ocean, and subsidence conditions in subtropical latitudes promoted by the active SACZ are key ingredients in the development of heat waves (Cerne and Vera 2011), the forecasts of the OLR and 200 hPa geopotential height anomalies for each week are addressed.

3.2 OLR

The observed weekly OLR anomalies and forecasted evolution during the heat wave for different lead times are shown in Figs. 5, 6 and 7. During week 1 of the heat wave intense negative OLR anomalies were observed over central Brazil and the SACZ region while positive OLR anomalies were observed over SESA (Fig. 5). These dipole-like anomalies span the regions where the leading mode of OLR in intraseasonal timescales (e.g., Gonzalez and Vera 2014) exhibits more variability. The POAMA model captured some of this features in the forecasted OLR anomalies since lead 12, while the BCC-CPS model forecasted negative OLR anomalies over the SACZ region since lead 22 (Fig. 5). However, the spatial structure of these negative anomalies is not similar to that observed, particularly over the continent. Also, both models showed a large positive center of OLR anomalies in the northeast of the continent, which was not observed to be as large during that week.

During week 2, the intense SACZ remained developed (Fig. 6). The POAMA model only seemed to detect this SACZ for lead 19, though considerably weaker; and lead 4, though the oceanic SACZ portion could not be forecasted. On the other hand, the BCC-CPS forecasted a weaker than observed SACZ for leads 14 and 9, and a pattern more similar to the observations for lead 4 (Fig. 6). In contrast, the last week of the heat wave was not accompanied by an active SACZ: convection was enhanced over central and northeastern Argentina, Uruguay and southeastern Brazil, which was better forecasted by both models for longer leads (Fig. 7). Also, during this week, positive anomalies of OLR were observed over the oceanic portion of the SACZ but not over eastern Brazil. This pattern was forecasted by POAMA since lead 11, but was not represented by the BCC-CPS model (Fig. 7). Therefore, the performance of the BCC-CPS for leads 6 and 1 was worse than POAMA's, though neither could represent the enhanced convection in SESA during this week.

3.3 Geopotential height

The 200 hPa geopotential height anomalies observed during the weeks of the heat wave and those forecasted by POAMA and BCC-CPS models are presented in Figs. 8, 9 and 10. During the first week of the heat wave, an anticyclonic anomaly located over the southern tip of the continent (Fig. 8) promotes subsidence conditions north of northern Patagonia. The POAMA model forecasted the strongest anomaly in that region for lead 12, which may explain the intense warm anomalies forecasted for that lead (Fig. 1), and for leads 17 and shorter the model was also able to predict a positive anomaly in that region. The BCC-CPS model forecasted the anticyclonic anomaly south of where it was observed (Fig. 8), which might be related to the prediction of the positive temperature anomalies over the Patagonia (Fig. 1). The anomaly resulted more intense for leads 7 and 2, being the latter more similar to the observed anomalies, probably part of the reason why the location of the warm temperature anomalies was also more similar to that observed (Fig. 1). The wavetrain observed along the South Pacific extended between 30S and 65S, and was better represented by the

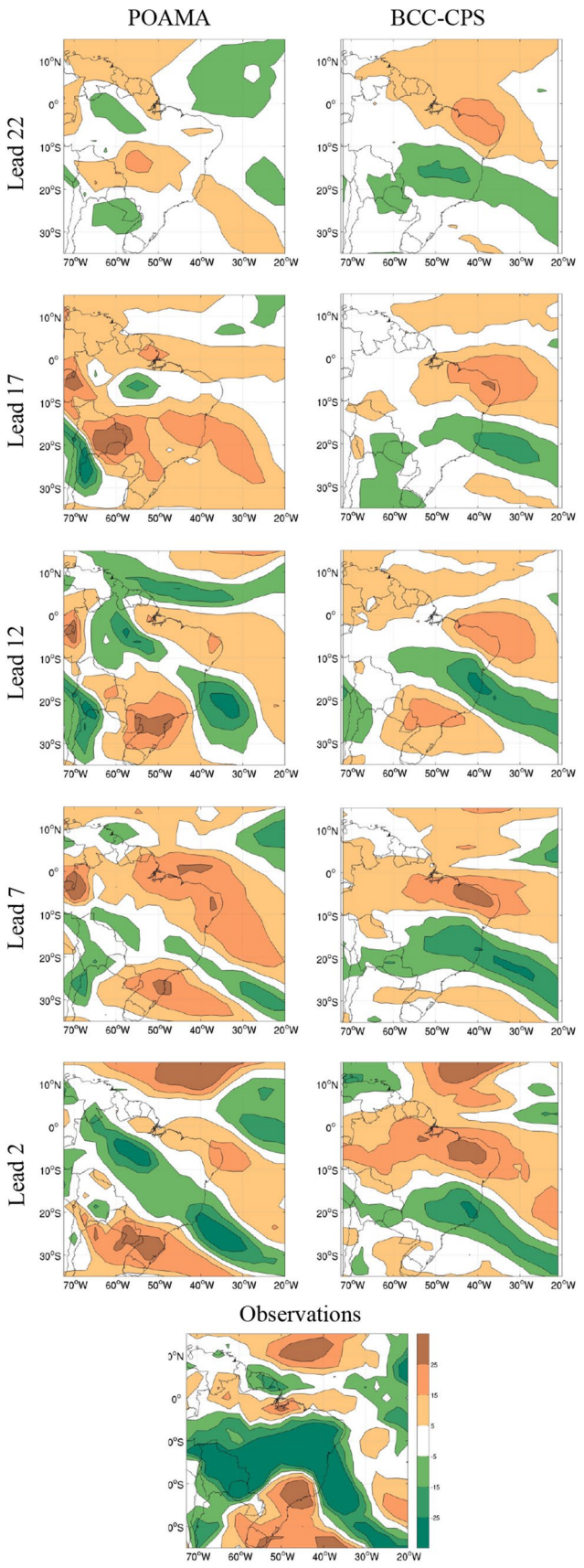

Fig. 5 Reforecasts of weekly-averaged OLR anomalies for POAMA ▸ model (*up*) and BCC-CPS (*down*) for week 1 of the heat wave (13 to 19 of December of 2013). The lead time indicates how many days before of the 1st day of the week the forecast started. Satellite-derived OLR anomalies for week 1 are shown at the *bottom*. Units are in W/m^2

POAMA model since lead 7 and also lead 12 between the date line and South America (Fig. 8). The BCC-CPS model generated a marked wavetrain since lead 7, though the anomalies resulted somewhat displaced to the south (Fig. 8).

On week 2 an intense upper-level anticyclonic anomaly was observed over central Argentina (Fig. 9), which was forecasted—though with less intensity—by the POAMA model for every lead since 24, possibly contributing to the forecasted warm anomalies (Fig. 2). The BCC-CPS model, on the other hand, only forecasted the anticyclonic anomaly over central Argentina for leads 4 and 9, while for leads 24 and 14 it was forecasted more to the south (Fig. 9), as were the temperature anomalies for those leads (Fig. 2). For this week the wavetrain does not seem to have been correctly predicted by neither of the models. In this sense, other studies have shown that even though models are able to reproduce wavetrains emanated from tropical oceans over the western and central Pacific and the Antarctic peninsula, they might not be accurately captured over South America (Osman 2017). However, it is remarkable that the strong anticyclonic anomaly located in subpolar latitudes and 130W could be forecasted by the POAMA model since lead 24 (Fig. 9).

The circulation anomalies over South America were more zonally-oriented during week 3 of the heat wave: a cyclonic anomaly over the South Atlantic Ocean extending towards South America and an anticyclonic one to the north (Fig. 10). This pattern was forecasted by both models for lead 1, though the POAMA model could only represent the cyclonic anomaly for lead 6, which was observed more to the east for longer leads. This is coherent with the cold anomalies forecasted in the South Atlantic Ocean by POAMA, as this cyclonic anomaly is mostly barotropic-equivalent (not shown) and therefore might be responsible for cold advection from subpolar latitudes. For this week, as opposed to the POAMA model, the BCC-CPS forecasted an anticyclonic anomaly over central Argentina since lead 11 (Fig. 10), possibly contributing to the better location of the warm anomalies observed in Fig. 3 for this model. The upper-level circulation anomalies along the South Pacific Ocean were for this week better forecasted by the POAMA model, though only up to lead 6, while longer leads do not resemble the wavetrain observed (Fig. 10).

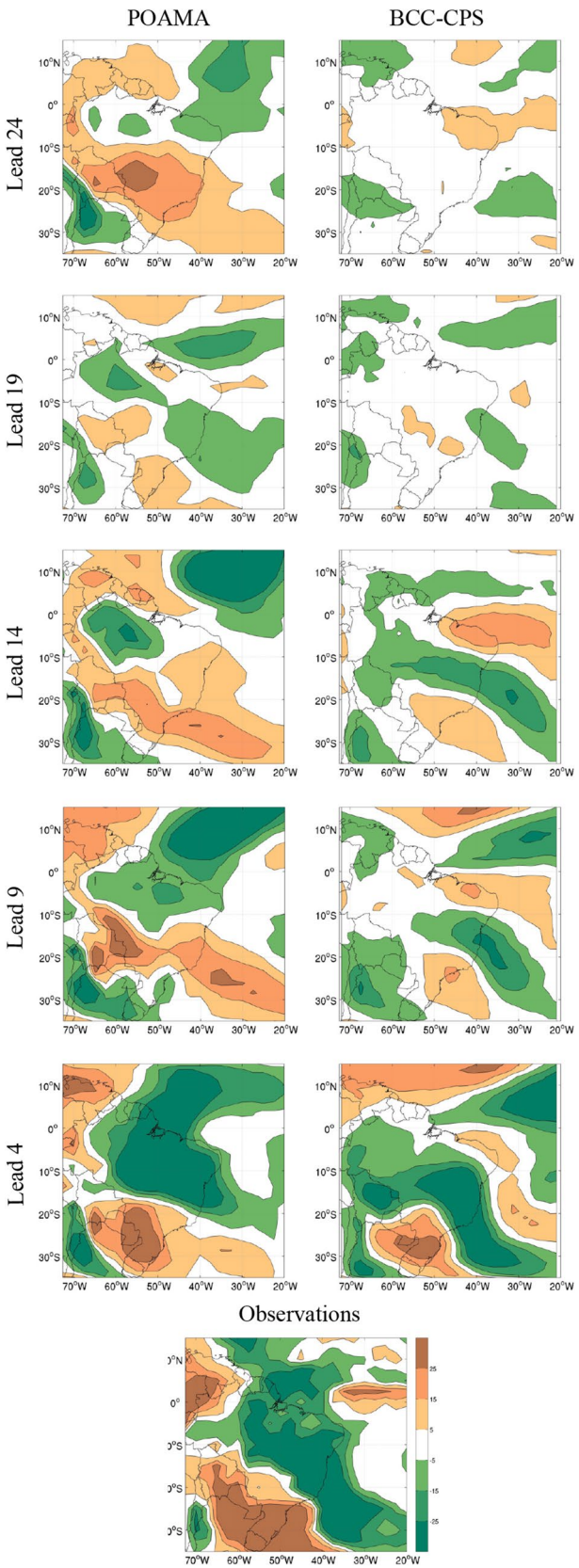

Fig. 6 As Fig. 5 but for week 2 of the heat wave (20 to 26 of December of 2013)

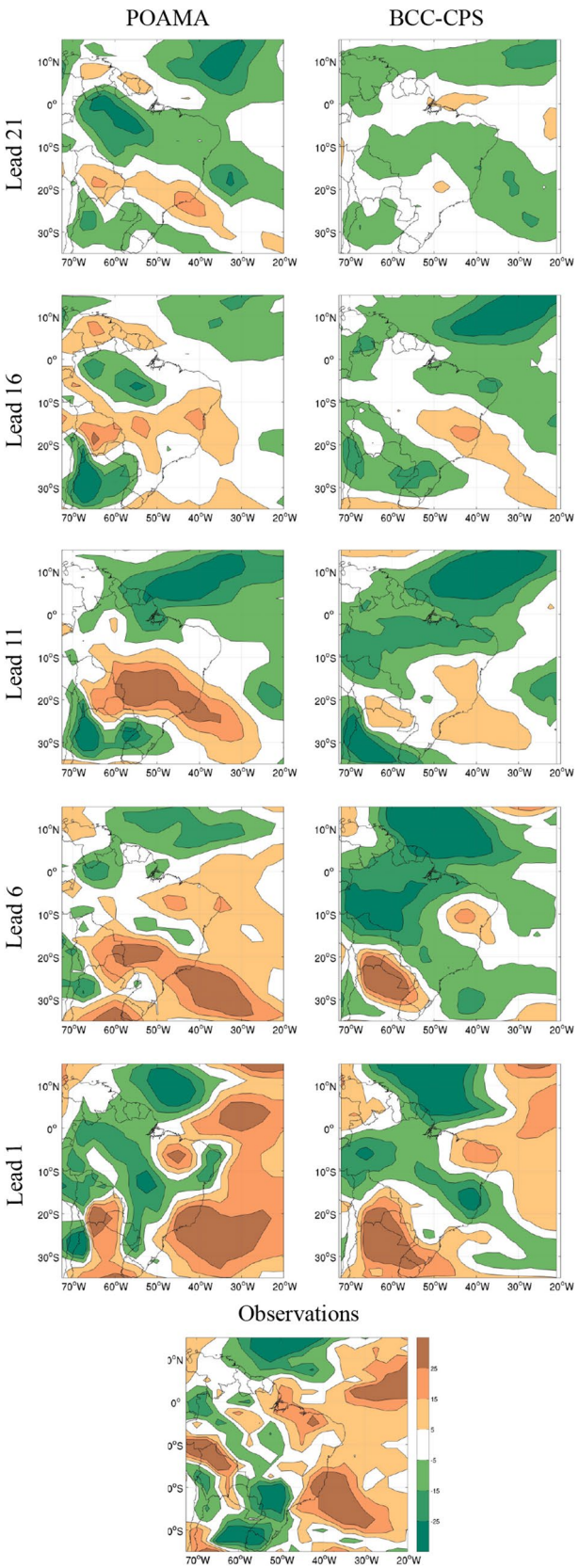

Fig. 7 As Fig. 5 but for week 3 of the heat wave (27 to 31 of December of 2013)

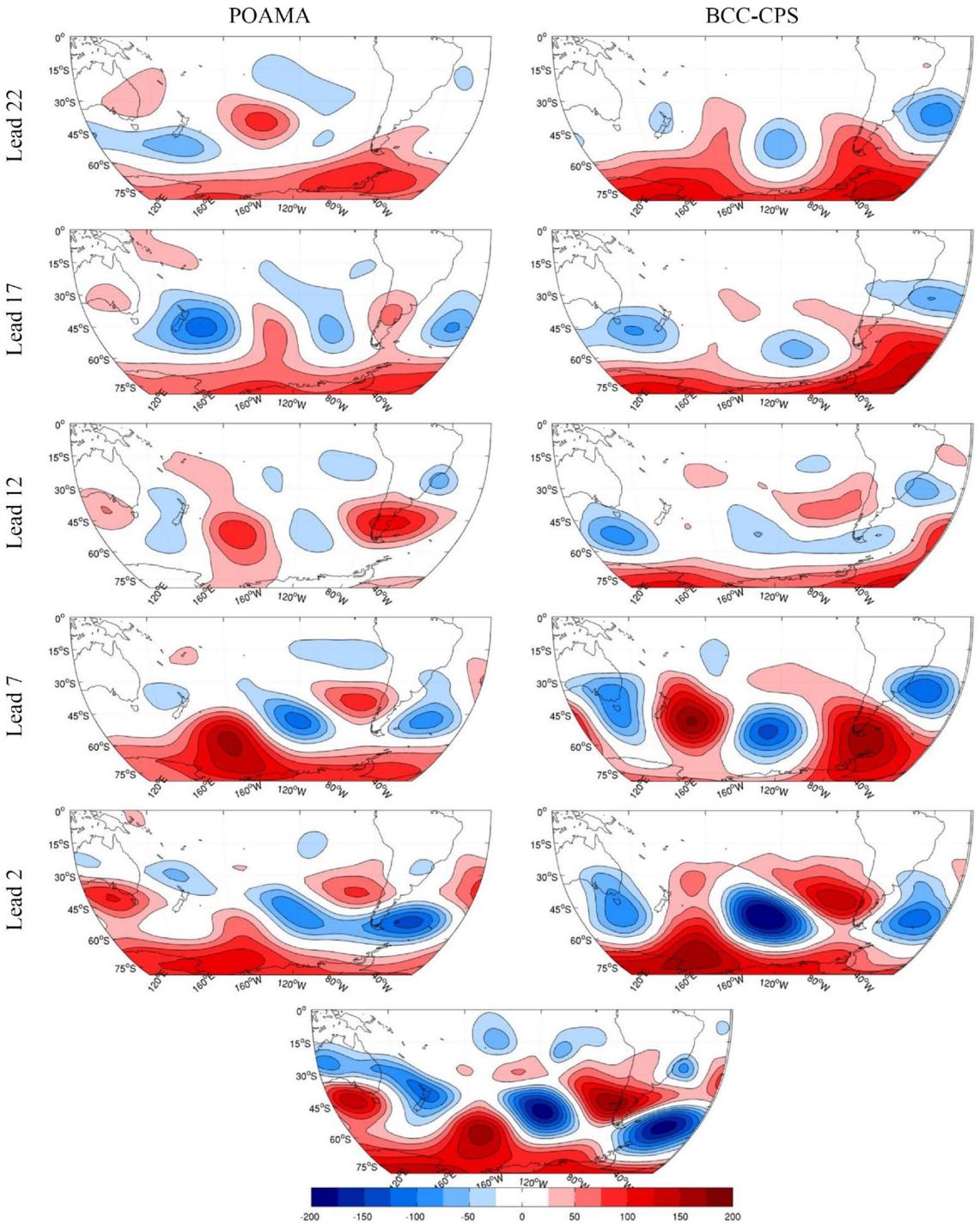

Fig. 8 Reforecasts of weekly-averaged 200 hPa geopotential height anomalies for POAMA model (*left*) and BCC-CPS (*right*) for week 1 of the heat wave (13 to 19 of December of 2013). The lead time indicates how many days before of the 1st day of the week the forecast started. Observations for week 1 are shown at the *bottom*. Units are in m

4 Summary and conclusions

In this paper we analyzed the subseasonal forecast for an intense heat wave event that took place in Southern South America during December 2013 with two models available in the database of the S2S project of the WWRP/WCRP: the POAMA model of the Australian Bureau of Meteorology and the BCC-CPS of the Chinese Meteorological Agency.

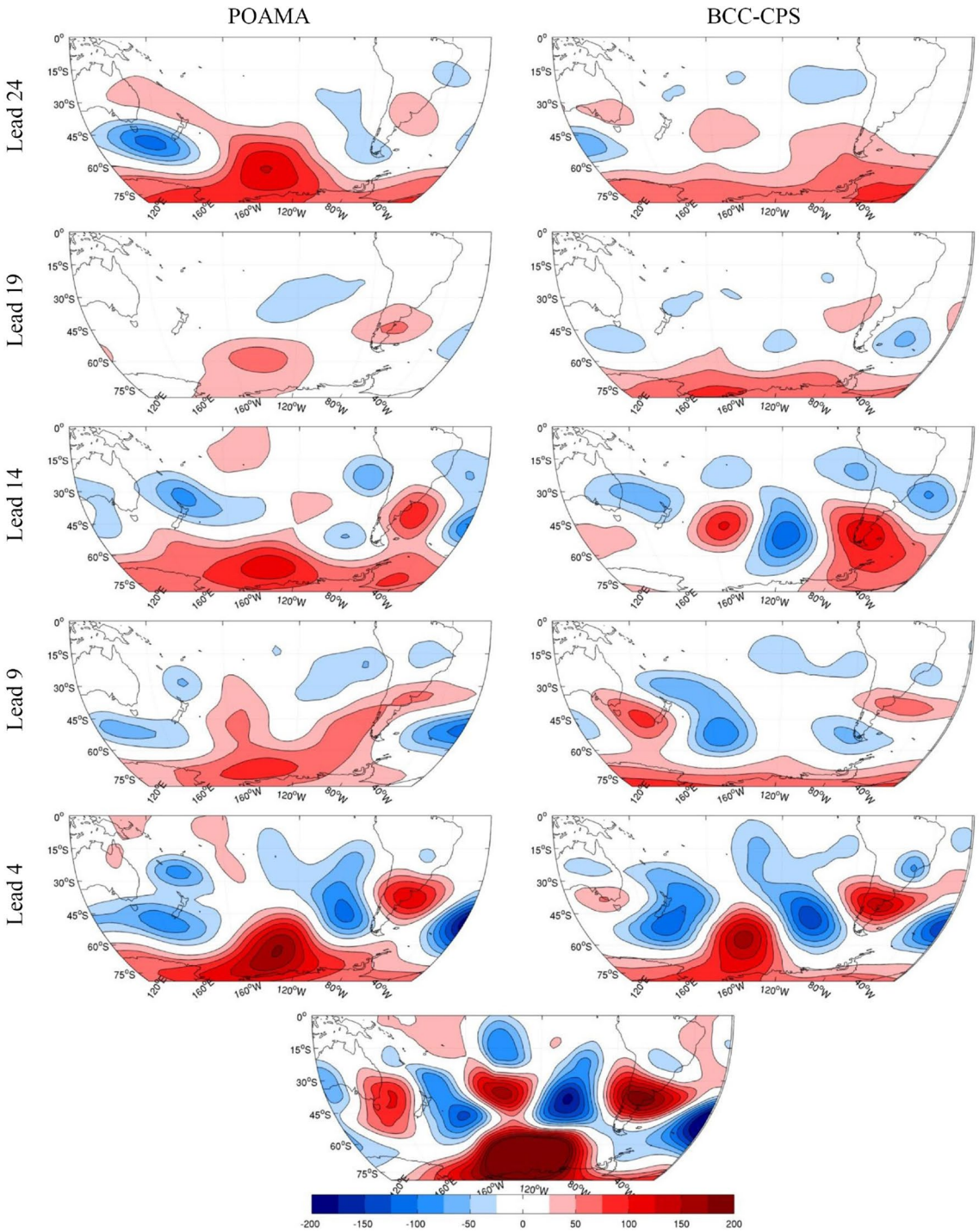

Fig. 9 As Fig. 8 but for week 2 of the heat wave (20 to 26 of December of 2013)

The ensemble mean warm anomalies forecasted for week 1 and 2 of the heat wave resulted more similar to the observations for the POAMA model, particularly for longer leads, while the BCC-CPS only forecasted patterns similar to those observed for leads shorter than 7 (14) for week 1 (2). For shorter leads, the skill scores also reveal that both models perform similarly, and the BCC-CPS better than POAMA for week 2. For week 3 the BCC-CPS outperformed the POAMA model, locating more accurately the maxima of the anomalies for the shorter leads, reaching better skill scores. The analysis of the ensemble spread reveals that while it reduces considerably with shorter

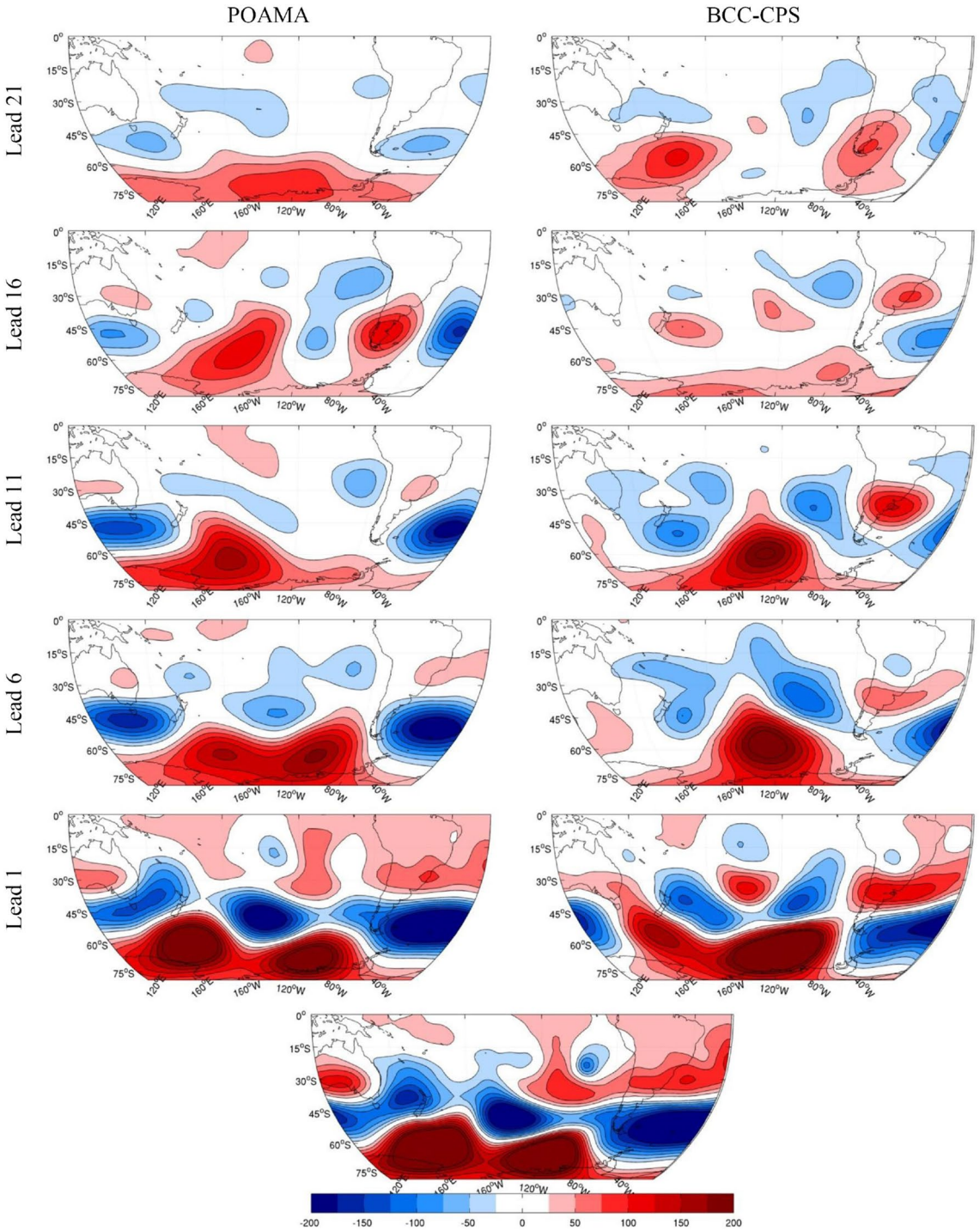

Fig. 10 As Fig. 8 but for week 3 of the heat wave 3 (27 to 31 of December of 2013)

leadtimes for BCC-CPS it remains almost unchanged for POAMA, especially for week 1 and 2. This is also observed when the scores for the ensemble members are analyzed.

The warm anomalies forecast was also analyzed probabilistically, as the chance of exceeding the 75th percentile within the region of highest anomalies. This analysis revealed that POAMA considerably outperformed the BCC-CPS, predicting higher than nominal chances for every lead of weeks 2 and 3 and leads 22 and 12 of week 1, while the BCC-CPS does for the shorter leads. In this way, the POAMA model resulted more effective in

the probabilistic forecast of the heat wave for lead times longer than the fortnight.

We also analyzed the performance of the models in forecasting the dynamic mechanism described by Cerne and Vera (2011) for this type of heat waves. The forecast of an active SACZ was better in the BCC-CPS model for weeks 1 and 2, though the spatial pattern resulted only similar to that observed for the shortest lead. On the other hand, the regional upper-level circulation was better forecasted by the POAMA model consistently since the longer leads during week 1 and 2, which might have been related to the better forecast of warm anomalies for weeks in advance.

The analysis done in this work reveals that both POAMA and BCC-CPS models had some skill to forecast this heat wave for ranges beyond the weather and might have potential to be used in the prediction of this type of extreme events. However, our study included very few models available in S2S database and was limited to model-to-model analysis. There are several works that show the advantages of the multi-model ensemble (MME) strategy over the single model one in multiple aspects (e.g. Hagerdorn et al. 2005). Hence, future works are needed to assess the performance of a subseasonal MME in forecasting extreme events.

Acknowledgements This work is based on S2S data. S2S is a joint initiative of the World Weather Research Programme (WWRP) and the World Climate Research Programme (WCRP). The original S2S database is hosted at ECMWF as an extension of the TIGGE database. We acknowledge The World Meteorological Organization and The International Centre for Theoretical Physics which have supported this work through the organization of the "Advanced School and Workshop on Subseasonal to Seasonal Prediction and Application to Drought Prediction". The research was supported by CONICET/PIP 112-20120100626CO, UBACyT 20020130100489BA, PIDDEF 2014/2017 Nro 15, and the CLIMAX Project funded by Belmont Forum. MSA is supported by a PostDoc grant from CONICET, Argentina. MO is supported by a Ph.D. grant from CONICET, Argentina.

References

Barros VR, Boninsegna JA, Camilloni IA, Chidiak M, Magrín GO, Rusticucci M (2015) Climate change in Argentina: trends, projections, impacts and adaptation. Wiley Interdiscip Rev Clim Change 6(2):151–169. doi:10.1002/wcc.316

Brown BG, Gilleland E, Ebert EE (2011) Forecasts of spatial fields. Wiley, New York, pp 95–117. doi:10.1002/9781119960003.ch6

Cerne SB, Vera CS (2011) Influence of the intraseasonal variability on heat waves in subtropical South America. Clim Dyn 36(11–12):2265–2277

Cerne B, Vera C, Alvarez M (2015) Influencia de la variabilidad intraestacional en el desarrollo de la ola de calor de diciembre de 2013 en el este de Sudamérica. In: Congreso Argentino de Meteorología (CONGREMET) XII

Cottrill A, Hendon HH, Lim EP, Langford S, Shelton K, Charles A, McClymont D, Jones D, Kuleshov Y (2013) Seasonal forecasting in the Pacific using the coupled model POAMA-2. Weather Forecast 28(3):668–680. doi:10.1175/WAF-D-12-00072.1

Dee DP, Uppala SM, Simmons AJ, Berrisford P, Poli P, Kobayashi S, Andrae U, Balmaseda MA, Balsamo G, Bauer P, Bechtold P, Beljaars ACM, van de Berg L, Bidlot J, Bormann N, Delsol C, Dragani R, Fuentes M, Geer AJ, Haimberger L, Healy SB, Hersbach H, Hólm EV, Isaksen L, Kållberg P, Köhler M, Matricardi M, McNally AP, Monge-Sanz BM, Morcrette JJ, Park BK, Peubey C, de Rosnay P, Tavolato C, Thépaut JN, Vitart F (2011) The ERA-Interim reanalysis: configuration and performance of the data assimilation system. Q J R Meteorol Soc 137(656):553–597. doi:10.1002/qj.828

Gonzalez PLM, Vera CS (2014) Summer precipitation variability over South America on long and short intraseasonal timescales. Clim Dyn 43(7):1993–2007. doi:10.1007/s00382-013-2023-2

Griffies SM, Gnanadesikan A, Dixon KW, Dunne JP, Gerdes R, Harrison MJ, Rosati A, Russell JL, Samuels BL, Spelman MJ, Winton M, Zhang R (2005) Formulation of an ocean model for global climate simulations. Ocean Sci 1(1):45–79. doi:10.5194/os-1-45-2005

Hagerdorn R, Doblas-Reyes FJ, Palmer TN (2005) The rationale behind the success of multi-model ensembles in seasonal forecasting—I. Basic concept. Tellus A 57(3):219–233. doi:10.1111/j.1600-0870.2005.00103.x

Hannart A, Vera C, Cerne B, Otto FEL (2015) Causal influence of anthropogenic forcings on the Argentinian heat wave of December 2013. Bull Am Meteorol Soc 96(12):S41–S45. doi:10.1175/BAMS-D-15-00137.1

Hudson D, Marshall AG, Yin Y, Alves O, Hendon HH (2013) Improving intraseasonal prediction with a new ensemble generation strategy. Mon Weather Rev 141:4429–4449. doi:10.1175/MWR-D-13-00059.1

Liebmann B, Smith C (1996) Description of a complete (interpolated) outgoing longwave radiation dataset. Bull Am Meteorol Soc 77:1275–1277

Liu X, Wu T, Yang S, Li T, Jie W, Zhang L, Wang Z, Liang X, Li Q, Cheng Y, Ren H, Fang Y, Nie S (2016) MJO prediction using the sub-seasonal to seasonal forecast model of Beijing Climate Center. Clim Dyn. doi:10.1007/s00382-016-3264-7

Marshall AG, Hendon HH (2015) Subseasonal prediction of Australian summer monsoon anomalies. Geophys Res Lett 42(24):10913–10919. doi:10.1002/2015GL067086

Osman M (2017) Predictability and prediction skill on seasonal timescales over South America. Ph.D. thesis, Universidad de Buenos Aires. Facultad de Ciencias Exactas y Naturales (to be published)

SMN (2014) Informe especial debido a la ocurrencia de una ola de calor excepcional en argentina durante diciembre de 2013. Technical report. http://www.smn.gov.ar/serviciosclimaticos/clima/archivo/informe_temperatura_dic13.pdf

Vitart F, Ardilouze C, Bonet A, Brookshaw A, Chen M, Codorean C, Déqué M, Ferranti L, Fucile E, Fuentes M, Hendon H, Hodgson J, Kang H, Kumar A, Lin H, Liu G, Liu X, Malguzzi P, Mallas I, Manoussakis M, Mastrangelo D, MacLachlan C, McLean P, Minami A, Mladek R, Nakazawa T, Najm S, Nie Y, Rixen M, Robertson AW, Ruti P, Sun C, Takaya Y, Tolstykh M, Venuti F, Waliser D, Woolnough S, Wu T, Won DJ, Xiao H, Zaripov R, Zhang L (2016) The sub-seasonal to seasonal prediction (S2S) project database. Bull Am Meteorol Soc. doi:10.1175/BAMS-D-16-0017.1

Wilks D (2011) Statistical methods in the atmospheric sciences. Academic Press, Oxford. https://books.google.com.ar/books?id=IJuCVtQ0ySIC

Wu T (2012) A mass-flux cumulus parameterization scheme for large-scale models: description and test with observations. Clim Dyn 38(3):725–744. doi:10.1007/s00382-011-0995-3

Wu J, Ren HL, Zuo J, Zhao C, Chen L, Li Q (2016) MJO prediction skill, predictability, and teleconnection impacts in the Beijing Climate Center Atmospheric General Circulation Model. Dyn Atmos Oceans 75:78–90. doi:10.1016/j.dynatmoce.2016.06.001

Yin Y, Alves O, Oke PR (2011) An ensemble ocean data assimilation system for seasonal prediction. Mon Weather Rev 139(3):786–808. doi:10.1175/2010MWR3419.1